Reduction of the Coherence Time of an Intense Laser Pulse Propagating through a Plasma

J. Fuchs, C. Labaune, H. Bandulet, and P. Michel*
Laboratoire pour l'Utilisation des Lasers Intenses, UMR No. 7605 CNRS-École Polytechnique-CEA-Université Paris VI, École Polytechnique 91128 Palaiseau Cedex, France

S. Depierreux
CEA-DIF, BP 12, 91680 Bruyères-Le-Châtel, France

H. A. Baldis
Institute for Laser Science and Applications, Lawrence Livermore National Laboratory, Livermore, California 94550
(Received 27 November 2001; published 25 April 2002)

We present direct measurements of the coherence time of a laser beam after propagation through an underdense plasma. At an intensity of 10^{14} W/cm^2, a large decrease of the coherence time is observed, from 300 ps to a few picoseconds. This decrease is larger as the plasma density is increased or as the light is scattered at larger angles. The amount of temporal decorrelation as well as the effect of the plasma density, laser intensity, and scattering angle all coincide with trends observed in recent numerical simulations.

DOI: 10.1103/PhysRevLett.88.195003 PACS numbers: 52.35.Mw, 42.25.Kb, 52.38.–r, 52.70.Kz

The control of coherence is a critical issue for the high-power lasers used in inertial confinement fusion (ICF). Speckled focal patterns commonly produced by these lasers induce detrimental effects for ICF such as the degradation of the required irradiation uniformity [1] or the growth of laser-plasma instabilities (LPI) [2]. Significant control of the focal spot properties has been gained over the last two decades using techniques that modify the lasers' coherence such as random phase plates (RPP) [3] or smoothing by spectral dispersion (SSD) [4]. However, recent theoretical [5–11] and experimental [12–15] studies have shown that coherence could also be altered by the coupling of the laser beams with an underdense plasma. As a result, such plasma-induced incoherence (PII) can lead to uncontrolled significant modifications of the focal spot intensity distribution inside the plasma and therefore can affect the expected LPI growth.

PII proceeds from several mechanisms which include self-focusing [2] and filament [6] instabilities and nonlinear coupling between self-focusing and forward stimulated Brillouin scattering (FSBS) [5,9,11]. This effect could be a major issue in the prospect of achieving ignition in the future mega-Joule scale ICF facilities, particularly for the indirect drive where long path lengths of underdense plasma are involved [1] since, on the one hand, it may angularly redistribute the energy, but on the other hand, by reducing the coherence of the beam, it may lower the growth of LPI.

Reports of PII have relied so far on indirect signatures, such as spectral bandwidth or angular divergence [12–15]. In this Letter, we present the first direct measurements, using a Michelson interferometer, of the coherence time of an initially RPP-smoothed laser beam, propagating in a well-characterized, long, underdense plasma. We observe a strong reduction of the coherence time from ~300 to ~4–20 ps, depending on the laser beam intensity, the plasma density, and the forward scattering angle. These results, well correlated with the spectral bandwidth of the forward scattered light, show quantitatively that (i) PII outreaches present SSD in reducing the coherence time [4,8,16] and that (ii) PII is therefore likely to have a significant impact on the growth of SBS. They are in good agreement with recent numerical simulations [8,9].

The experiment is performed using four beams of the LULI (Laboratoire pour l'Utilisation des Lasers Intenses) laser facility. All beams are in the horizontal plane with 600 ps FWHM (full width at half maximum) Gaussian pulses. The plasma is formed by two counterpropagating, 526 nm wavelength laser beams incident on 380 μm diameter freestanding CH (parylene N) disks of thickness 1.2 μm, and heated by a third, identical beam, delayed by 0.6 ns with respect to the first two. These beams are propagated through RPPs that produce a focal spot larger than the target. The $\lambda = 1.053$ μm wavelength interaction beam is focused, through a 2 mm element RPP, with a $f/6$ optic along the principal axis of plasma expansion and delayed by 1.6 ns with respect to the plasma formation pulses. The speckle distribution in the focal spot [17] has a diameter (at FWHM) of 320 μm, producing a peak average intensity of $\langle I_{14} \rangle \sim 1$ in units of 10^{14} W/cm^2.

The resulting plasma has well-known characteristics [18]. Electron temperatures range between 0.5 and 0.7 keV during the interaction pulse. The electron density at the top of the plasma profile decreases exponentially in time $n_{\mathrm{top}}(t)/n_c \sim 0.13 \exp(-t[\mathrm{ps}]/530)$, where $n_c = 1.1 \times 10^{21}$ cm^{-3} is the critical electron density at λ_0 and $t = 0$ corresponds to the peak of the interaction pulse. The typical scale length of the plasma's parabolic profile is

700 μm. By lowering the energy of the plasma-formation beams, higher plasma densities, namely, $n_{\text{top}}(t = 0) \sim 0.6n_c$, are also used in our experiments.

Two optics are used to collect the light of the interaction beam that is forward scattered. The first one is on axis with an aperture twice the one of the incident interaction beam. It collects light scattered at $0° \pm 10°$ with respect to the interaction beam axis. The second one is placed off axis to collect light scattered at $22.5° \pm 5°$. A diagnostic station measures the time-resolved spectra of the forward scattered light, using a spectrometer-streak camera combination, with spectral and temporal resolutions of 2 Å and 150 ps, respectively. For the direct measurement of the coherence time, the near field in the collecting optics' plane is image relayed onto the mirrors of a Michelson interferometer that is set in an air-wedge configuration. The produced pattern of straight parallel fringes is imaged onto a streak camera having a temporal resolution of ~30 ps. The relative positioning of the streak camera's slit within the near-field plane of the collecting optics that is imaged up to the streak camera provides angular resolution for the coherence measurement: since the slit (placed perpendicular to the fringes) sees only a well-defined part of the near field, it defines the angular range of the forward scattered light over which the measurement is made. When the two replicas of the pulse produced by the interferometer superimpose in time, perfect fringes are observed during the whole pulse evolution. However, when a delay Δt between the two replicas is introduced, the fringes are blurred if, during the pulse evolution, there is temporal incoherence between the times t and $t + \Delta t$. By scanning the delays, and by streaking the interference pattern for each delay, we are able to measure the time dependence of the coherence time within the temporal evolution of the pulse. Experimentally, we define the coherence time (τ) as the delay Δt for which the fringes' visibility, $V = [I_{\max} - I_{\min}]/[I_{\max} + I_{\min}]$, is below 0.1. With this diagnostic used through vacuum, we measure the initial laser's coherence time as ~300 ps.

When the interaction beam is propagated at high intensity ($\langle I_{14} \rangle \sim 1$) through the $\sim 0.1n_c$, ~1 mm long plasma, its coherence time is greatly reduced, as shown in Fig. 1. The selected light is collected, at 7°, outside the incident cone. For $\Delta t = 0$ (± 2) ps (see Fig. 1a), we observe, as expected, fringes with a good constant visibility. However, as soon as $\Delta t = 8$ ps (see Fig. 1b), the fringes, which are clear at the beginning and at the end of the pulse, are blurred ($V \sim 0.15$) between $t = 100$ and 300 ps after the peak of the pulse. This means that, for this part of the pulse, the coherence time has been reduced to near 8 ps. If we further increase Δt to 18 ps (see Fig. 1c), we see that the blurring is complete ($V \leq 0.1$) from $t = -100$ ps to the end of the pulse. For all this temporal range, the coherence time is therefore $\leq$18 ps.

The varying visibility of the fringes over time shows that the coherence time varies within the output laser pulse.

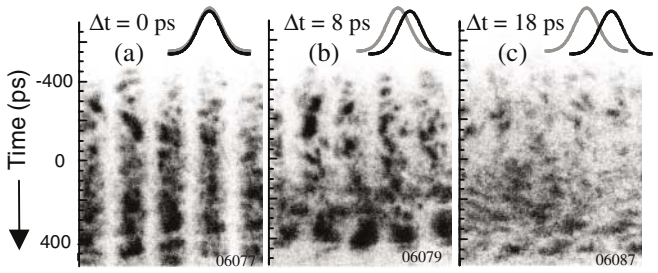

FIG. 1. (a) Time-resolved fringe pattern in the output of the Michelson interferometer for light scattered at 7° from the incident axis (outside the incident cone) after propagation at high intensity ($\langle I_{14} \rangle \sim 1$) through a $\sim 0.1n_c/1$ mm plasma and with a delay $\Delta t = 0 \pm 2$ ps between the two replicas. Time 0 corresponds to the peak of the incident pulse. (b) The same with $\Delta t = 8$ ps. (c) The same with $\Delta t = 18$ ps. The fine structure within the dark fringes corresponds to spatial structures within the near-field scattered light and not to an interference effect.

This may be seen as an intensity effect since the pulse has a Gaussian temporal dependence in intensity. Such intensity dependence of the output coherence time is confirmed by repeating the same experiment with varying laser intensities as shown in Fig. 2. The visibility of the fringes improves as the laser intensity is lowered down to 10^{11} W/cm^2 at which value clear constant fringes are observed (see Fig. 2c). These results also show that the reduction of the temporal coherence of the laser beam appears at a low intensity threshold.

For light scattered further outside the incident aperture, the coherence time is even more reduced. As shown in Fig. 3, for light scattered at four times the incident aperture (22°), the fringes are already blurred, at all times, for $\Delta t = 4$ ps, meaning that $\tau \leq 4$ ps. This coherence time is lower than the one observed at 7° and indeed the pattern produced, at the same delay, by light scattered at 7° exhibits no decrease of visibility. Conversely, within the incident cone, the coherence time is longer (~17 ps). This is shown in Fig. 3c where we plot, for light scattered at three different angles inside and outside the incident cone, the minimum recorded visibility (i.e., around the peak of the pulse) as a function of the delay Δt in the interferometer.

The induced incoherence is also favored by an increase in the plasma density. When the density at the peak of the

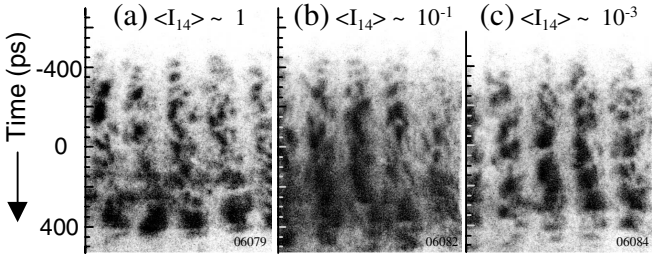

FIG. 2. Fringe pattern, recorded in the same conditions as in Fig. 1b, for varying incident intensity: $\langle I_{14} \rangle \sim 1$ in (a), 10^{-1} in (b), and 10^{-3} in (c).

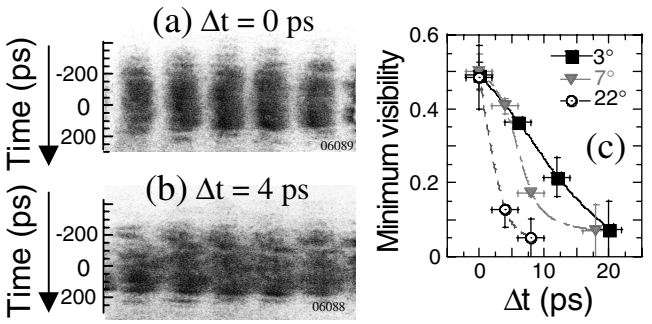

FIG. 3. (a) Fringe pattern recorded in the same conditions as in Fig. 1 but for light scattered at 22°, far outside the incident beam aperture and for $\Delta t = 0$ ps, (b) the same with $\Delta t = 4$ ps, and (c) variation of the fringes' minimum visibility as a function of Δt and for three different scattering angles.

pulse goes from $\sim 0.1 n_c$ to $\sim 0.6 n_c$, the fringe pattern at $\Delta t = 8$ ps starts blurring sooner and has a lower visibility than what can be seen in Fig. 1b. At this density, the decrease of the coherence time is also larger as the light sprays at wider angles.

The spectral features of the forward scattered light are in excellent agreement with the direct measurement of the coherence time. The spectrum of the light, shown in Fig. 4a, recorded in the same conditions as in Fig. 1 exhibits two components: (i) one that, within the resolution, is in agreement with the shift predicted by classical SBS [2] ($\sim$0.5 Å at this angle) and (ii) a redshifted (up to 10 Å) wing that appears around the peak of the laser pulse with a shift slowly decreasing in time to reduce to the incident linewidth by the end of the pulse. The connection with the coherence measurements is done through the Wiener-Khintchine theorem [19] which states that the Fourier transform of the power spectrum is equal to the variation of the visibility as a function of Δt, i.e., $V(t, \Delta t) \propto \int S(t, \nu) \exp(-2i\pi\nu\Delta t)\, d\nu$, where S is the measured time-resolved spectrum. In Fig. 4b, V is computed from the spectrum of Fig. 4a. At early times, $V(\Delta t)$ is a slowly decreasing function of Δt since the spectrum of the light is narrow whereas from $t \sim 0$ to the end of the pulse, $V(\Delta t)$ decreases much more rapidly due to the occurrence of spectral broadening. More precisely, following the contour at $V = 0.1$ of Fig. 4b, we see that, in the second half part of the pulse, τ is reduced between 18 ps (at $t = 0$ and $t = 450$ ps) and 10 ps (at $t = 170$ ps).

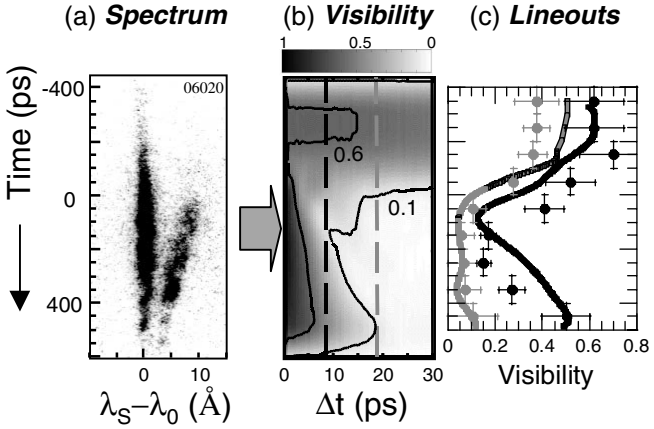

FIG. 4. (a) Time-resolved spectrum of the light scattered in the same conditions as in Fig. 1. (b) Time-resolved visibility, as calculated by Fourier transform of the spectrum displayed in (a), as a function of the delay Δt. Contours at $V = 0.6$ and 0.1 are superimposed. (c) Plots, for $\Delta t = 8$ ps (black) and 18 ps (gray), of the visibility temporal evolution obtained (i) following the dashed lines in (b) (lines) and (ii) from Figs. 1b and 1c (dots). The same vertical time scale applies for the three figures.

In order to better compare the Michelson and the spectral measurements, we plot for each method the visibility as a function of time for two delays (8 and 18 ps). The black and gray dots in Fig. 4c are the visibility measured from the fringes of Fig. 1b and Fig. 1c, respectively. The black and gray lines in Fig. 4c are the visibility calculated from the spectrum of Fig. 4a following the dashed lines of Fig. 4b. The good agreement between the results of both methods demonstrates that the complementary interferometric and spectral measurements are well correlated.

Using both, we can thus determine the coherence time of the output interaction beam for a wide range of laser and plasma conditions, as shown in Fig. 5. The two plots of Fig. 5 summarize the trends observed in Figs. 2 and 3: the coherence time decreases (i) as the scattering angle increases, although less steeply at high plasma density, and (ii) as the beam intensity increases, although more rapidly at high plasma density. The minimum coherence time that we observe is $\sim$4 ps at high density and/or wide angle.

The experimental results are consistent with the mechanisms that are theoretically put forward for PII occurrence [5–11]. The scenario is the following: from early times on, where incident intensity is low and further reduced by absorption within the high density plasma, intensity increases up to the point where critical (threshold) powers for the self-focusing [2] and the filament [6] instabilities can

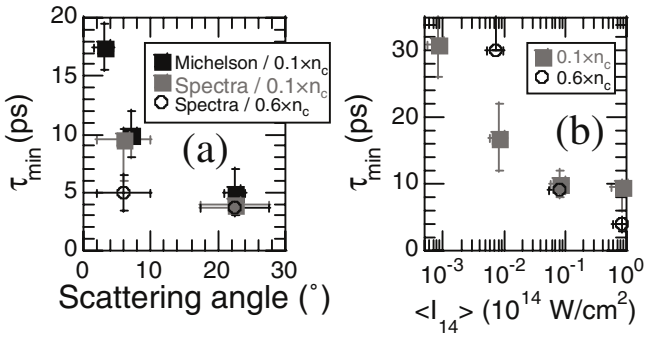

FIG. 5. Coherence time, measured around the peak of the pulse, for various plasma densities and (a) as a function of the angle at which the light is scattered forward (here $\langle I_{14} \rangle \sim 1$, constant) and (b) as a function of the incident intensity (here the light is collected at $\sim$6° from the beam axis, outside the incident cone).

be reached for some hot spots. Light then experiences fast phase changes, due to plasma expulsion within the self-focused filaments and strong growth of FSBS, that can be large enough to result in temporal decorrelation of a few picoseconds. After the peak of the pulse, intensity decreases and the rate of plasma digging and FSBS growth lowers, resulting in smaller phase perturbations (i.e., less reduction of the coherence time). When the plasma density is increased, the intensity needed to trigger PII is lower [10], which means that the coherence time of the pulse's low-intensity parts can be reduced much like the high-intensity parts, as seen in the experiment. Such a scenario and coherence times, well matched with experimental observations, have been seen in recent numerical simulations [8,9].

It is interesting to note that in simulations performed in conditions similar to ours (1 μm wavelength, $0.1n_c$ plasma density, 1 keV temperature, $f/4$ incident aperture) although at higher intensity ($\langle I_{14}\rangle \sim 7$) [9], the experimental trend of decreasing τ when the scattering angle increases is also observed. This trend is attributed to multiple FSBS (temporal correlation tends to be further reduced for scattered waves that are themselves the result of previous scattering). The discrepancy in intensity between the experiment and the simulations, according to which PII should not occur at $\langle I_{14}\rangle \sim 1$, may come from the fact that thermal effects which lower the critical power for the self-focusing instability [10,20,21] are not taken into account in the model of Ref. [9]. This is supported by the fact that the inclusion of the thermal contribution in the simulations performed in Ref. [10], which use the same parameters and the same intensity as ours, lead to an excellent agreement with our results, in the manifestations of PII. Thus, these thermal effects are likely to explain the low intensity threshold that we find in the experiment for the occurrence of PII.

The observed reduction of the coherence time may significantly affect the growth of backward SBS. From 2D far-field images of the interaction beam, we have observed that, in parallel with the coherence time reduction, the transverse size of the speckles is reduced, from ~ 9 μm (at low intensity) to ~ 5 μm (at high intensity). It is likely that the speckles have not only their transverse but also their longitudinal size reduced, as evidenced in the simulations [9]. Thus, shorter speckles will lead to smaller SBS gains. Moreover, it has been shown recently [22] that SBS can be dramatically reduced if the speckle pattern decorrelates in time before saturation occurs, i.e., if $\gamma_0 \tau \leq 10$ where γ_0 is the SBS mean growth rate [2]. As we have $\gamma_0 \sim 1\text{–}2$ ps^{-1}, this criterion is fulfilled in our conditions. Both experiments and simulations support the expected impact of PII on SBS as PII is observed to take place in the second part of the pulse (see Fig. 1) and seen numerically to occur in the rear part of the plasma profile [10]. This localization is opposite to that of backward SBS, which is seen to grow in the entrance part of the plasma and in the first half part of the pulse [18,23].

In summary, we have shown for the first time that the coherence time of a high-intensity laser beam after propagation through a long underdense plasma could be reduced to levels that are low enough to (i) meet what can be achieved by SSD and (ii) be likely to hamper significantly the subsequent growth of backward SBS. This also means that a correct understanding of past and future LPI experiments cannot be reached if PII is not taken into account. These observations provide for PII a complete set of quantitative data that can be used as benchmarks for models in order to, ultimately, examine the crucial issue of LPI control.

The authors gratefully acknowledge fruitful discussions with V. Tikhonchuk as well as the support of A. Michard and the technical groups of LULI. This work was performed under the auspices of the U.S. Department of Energy by University of California Lawrence Livermore National Laboratory, through the Institute for Laser Science and Applications, under Contract No. W-7405-ENG-48.

*Also at CEA-DIF, BP 12, 91680 Bruyères-Le-Châtel, France.

[1] J. Lindl, Phys. Plasmas **2**, 3933 (1995).
[2] W. Kruer, *The Physics of Laser-Plasma Interactions* (Addison-Wesley, New York, 1988).
[3] Y. Kato *et al.,* Phys. Rev. Lett. **53**, 1057 (1984).
[4] S. Skupsky *et al.,* J. Appl. Phys. **66**, 3456 (1989).
[5] V. V. Eliseev *et al.,* Phys. Plasmas **4**, 4333 (1997).
[6] D. Pesme *et al.,* Phys. Rev. Lett. **84**, 278 (2000).
[7] C. Still *et al.,* Phys. Plasmas **53**, 1057 (2000).
[8] G. Riazuelo and G. Bonnaud, Phys. Plasmas **8**, 1319 (2001).
[9] A. Maximov *et al.,* Phys. Plasmas **8**, 1319 (2001).
[10] J. Myatt *et al.,* Phys. Rev. Lett. **87**, 255003 (2001).
[11] A. Schmitt and B. Afeyan, Phys. Plasmas **5**, 503 (1998).
[12] P. Young *et al.,* Phys. Plasmas **2**, 2825 (1995).
[13] J. Moody *et al.,* Phys. Rev. Lett. **83**, 1783 (1999).
[14] C. Labaune *et al.,* C.R. Acad. Sci. Ser. IV, 727 (2000).
[15] J. Fuchs *et al.,* Phys. Rev. Lett. **86**, 432 (2001).
[16] J. Moody *et al.,* Phys. Rev. Lett. **86**, 2810 (2001).
[17] J. Garnier, Phys. Plasmas **6**, 1601 (1999).
[18] J. Fuchs *et al.,* Phys. Plasmas **7**, 4659 (2000).
[19] M. Born and E. Wolf, *Principles of Optics* (Pergamon Press, Oxford, 1975).
[20] A. Brantov *et al.,* Phys. Plasmas **5**, 2742 (1998).
[21] V. Tikhonchuk *et al.,* Phys. Plasmas **8**, 1636 (2001).
[22] P. Mounaix *et al.,* Phys. Rev. Lett. **85**, 4526 (2000).
[23] C. Labaune *et al.,* Phys. Rev. Lett. **76**, 3727 (1996).